Received: 14 Feb 2022 | **Accepted:** 17 Apr 2022
DOI: 10.54005/geneltip.1073349

ORIGINAL ARTICLE

The Appearances of Brain Metastases of Small Cell Lung Cancer on 18F-FDG PET/CT

Küçük Hücreli Akciğer Kanserinin Beyin Metastazlarının 18F-FDG PET/CT'deki Görünümleri

[1]Hasan Önner, [1]Farise Yilmaz, [2]Halil Özer, [2]Abdüssamet Batur, [1]Gonca Kara Gedik

[1]Selcuk University, Faculty of Medicine, Department of Nuclear Medicine, Konya, Turkey
[2]Selcuk University, Faculty of Medicine, Department of Radiology, Konya, Turkey

Correspondence

Hasan Önner, Associate Professor, M.D., Selcuk University, Faculty of Medicine, Department of Nuclear Medicine, Konya, Turkey

Email: hasanonner@gmail.com

How to cite ?

Önner H, Yılmaz F, Özer H, Batur A, Kara Gedik G. The Appearances of Brain Metastases of Small Cell Lung Cancer on 18F-FDG PET/CT. Genel Tıp Derg. 2022; 32(3): 272-275

ABSTRACT

Purpose: We evaluate the appearances of the brain metastases (BMs) detected by brain magnetic resonance imaging (MRI) of small cell lung cancer (SCLC) on 18Fluor-Fluorodeoxyglucose (18F-FDG) positron emission tomography/computed tomography (PET/CT).
Patients and methods: SCLC patients who had an 18F-FDG PET/CT scan and a brain MRI within 30 days for initial staging were included. MRI was used to detect BMs. The imaging results of BMs on 18F-FDG PET/CT were assessed. On the 18F-FDG PET/CT study, the BMs were classified as undetectable, hypometabolic, hypermetabolic, or mixed patterns (lesions with both hypermetabolic and hypometabolic parts).
Results: A total of 51 patients [48 (94.1%) of whom were male and 3 (5.9%) female, with an average age of 62.57 ± 9.64] were included in this study. Fifteen patients (29.4%) were in the limited stage, whereas 36 patients (69.6%) were in the extensive stage. In 11 individuals, MRI indicated 28 BMs. On 18F-FDG PET/CT, 13 of the 28 metastases were visible. The following were the BMs appearances on 18F-FDG PET/CT: hypometabolic (n: 4), hypermetabolic (n: 6), and mixed (n: 3). While the mean diameter of BMs detected in 18F-FDG PET/CT was 16mm; the mean diameter of undetected ones was 4.3 mm.
Conclusion: On 18F-FDG PET/CT, BMs can have a variety of appearances, including hypometabolic, hypermetabolic, and mixed patterns. On the other hand, failure to detect millimetric size BMs in 18F-FDG PET/CT prevents proper staging.

Key words: small cell lung cancer, positron emission tomography, brain metastasis

ÖZ

Amaç: Çalışmamızda, küçük hücreli akciğer kanserinin (KHAK) beyin manyetik rezonans görüntüleme (MRG) ile tespit edilen beyin metastazlarının (BM'ler) 18Fluor-Florodeoksiglukoz (18F-FDG) pozitron emisyon tomografisi/bilgisayarlı tomografisindeki (PET/BT) görünümlerini değerlendirdik.
Hastalar ve yöntem: Çalışmaya ilk evreleme amacıyla 30 gün içinde 18F-FDG PET/CT taraması ve beyin MRG'si olan SCLC hastaları dahil edildi. Beyin metastazlarını saptamak için MRG kullanıldı. BM'lerin 18F-FDG PET/BT üzerindeki görüntüleme bulguları değerlendirildi. 18F-FDG PET/BT çalışmasında BM'ler; saptanamayan, hipometabolik, hipermetabolik veya karışık (hem hipermetabolik hem de hipometabolik kısımları olan lezyonlar) paternler olarak sınıflandırıldı.
Bulgular: Çalışmaya yaş ortalaması 62.57 ± 9.64 olan 48'i (%94.1) erkek, 3'ü (%5.9) kadın; toplam 51 hasta dahil edildi. Hastaların 15'i (%29,4) sınırlı evredeyken, 36'sı (%69,6) yaygın evredeydi. 11 kişide, beyin MRG 28 BM gösterdi. 18F-FDG PET/BT'de 28 metastazın 13'ü görüldü. 18F-FDG PET/BT'deki BM görünümleri şunlardı: hipometabolik (n: 4), hipermetabolik (n: 6) ve karışık (n: 3). 18F-FDG PET/BT'de saptanan BM'lerin ortalama çapı 16mm iken; saptanamayanların ortalama çapı 4,3 mm idi.
Sonuç: 18F-FDG PET/BT'de BM'ler hipometabolik, hipermetabolik ve karışık paternler dahil olmak üzere çeşitli görünümlere sahip olabilir. Öte yandan, 18F-FDG PET/BT ile milimetrik boyutlu BM'lerin saptanamaması evrelemenin düzgün yapılmasını engellemektedir.

Anahtar Kelimeler: küçük hücreli akciğer kanseri, pozitron emisyon tomografisi, beyin metastazı

Introduction

Brain metastases (BMs) are found in about 20% of patients with small-cell lung cancer (SCLC) at diagnosis, whereas BM develops in 50-80% of patients during the course of the disease (1-3).

The role of Flour 18 Fluorodeoxyglucose (18F-FDG) positron emission tomography/computed tomography (PET/CT) in detecting BMs in SCLC has been evaluated in studies. According to the results of these studies, due to both its high physiological brain glycolytic activity and its relatively low resolution, 18F-FDG PET/CT has a lesser diagnostic capacity than magnetic resonance imaging (MRI) or computed tomography (CT) in detecting BMs (4, 5).

However, studies evaluating the appearance of BMs on 18F-FDG PET/CT in SCLC patients are limited (6-8). Hence, we devised our study to assess the appearance findings of BMs detected by brain MRI on initial staging 18F-FDG PET/CT in patients with SCLC.

Patients and methods

SCLC patients who had an 18F-FDG PET/CT scan and a brain MRI for initial staging at our hospital between January 2012 and December 2021 were analyzed retrospectively. Those with longer than 30 days interval between 18F-FDG PET/CT and brain MRI, those with secondary malignancies, those with previous

chemotherapy and radiotherapy, those with active or previous central nervous system infection, those with a previous cerebrovascular event, and those with MRI without contrast agent were all excluded from the study. Patients who met these specified criteria were included consecutively.

A brain MRI was used to diagnose BMs. The imaging findings of BMs indicated by brain MRI were evaluated using 18F-FDG PET/CT. The lung tumor is limited to one hemithorax and ipsilateral pleural effusion (negative cytology) was defined as "limited disease" and those not included in this group were defined as "extensive disease" according to the Modified Veterans Administration Lung Group (VALSG) classification used in clinical staging (9). With its decision dated 04.01.2022 and numbered 2022/03, the Selcuk University Faculty of Medicine Ethics Committee approved this study. The patients or their families submitted the informed consent form.

Imaging

PET/CT

From the vertex to the mid-thigh, PET/CT images were obtained with a scanner (Biograph mCT, Siemens, Germany) in a total of eight or nine-bed positions. Before receiving the injection of 18F-FDG (37Mbq/kg), all patients were requested to fast for at least six hours, and their blood glucose levels were confirmed to be less than 200 mg/dL. Low-dose CT without contrast was conducted 60 minutes after the injection using 16 slices of CT with 190 mA, 5 mm slice thickness, and 140 kV acquisition parameters for attenuation correction. The brain parenchyma window of CT and different scales of PET images were assessed to investigate the appearance of BMs identified in brain MRI. Considering normal cerebrum parenchyma, those that could not be distinguished were labelled undetectable, those with increased 18F-FDG uptake were marked hypermetabolic, and those with reduced 18F-FDG uptake were categorized hypometabolic, and those with both hypermetabolic and hypermetabolic components were classed as mixed. The study authors reached a compromise on the appearance patterns of the lesions.

Brain MRI

A 1.5 Tesla (Siemens Magnetom Area, Erlangen, Germany) scanner with head coils was used to conduct the brain MRI exams. The usual MRI protocol included susceptibility-weighted imaging, diffusion-weighted imaging, and T1 and T2-weighted imaging in various planes. All of the patients were given a gadolinium-based contrast agent (0.1 mmol/kg). All MRI sequences were used to diagnose BMs, particularly the post-contrast T1W scan. Long diameters on brain MRI were used for BMs size.

Statistical analysis

The patients' ages were given as mean ± standard deviation. The number of patients with BMs was indicated proportionately. The lesions observed in brain MRI during the 18F-FDG PET/CT scan were classified as undetectable, hypometabolic, hypermetabolic, or mixed (lesions with hypermetabolic and hypometabolic areas). All of these groups' proportional values were provided. The mean diameters of detectable and undetectable BMs were calculated.

Results

The data of 51 patients [48 males (94.1%) and three females (5.9%) (mean age: 62.57±9.64)] were analyzed. Fifteen patients (29.4%) were in the limited stage, whereas 36 patients (69.6%) were in the extensive stage. The data of the patients are given in Table 1. Figure 1 demonstrates the appearance of BMs detected by brain MRI on 18F-FDG PET/CT in a patient with SCLC.

Table 1. Demographic data of the patients

	n	%
Age (year)		
< 65	29	56.9
≥ 65	22	43.1
Sex		
Male	48	94.1
Female	3	5.9
Stage		
Limited	15	29.4
Extensive	36	69.6
Brain metastasis		
Yes	11	21.6
No	40	78.4

Table 2. The patterns of appearance of brain metastases on 18F-FDG PET/CT

	n	%
Undetectable	15	53.6
Hipometabolic	4	14.3
Hipermetabolic	6	21.4
Mixed	3	10.7

With brain MRI, BMs were found in 11/51 patients (21.6%). There were a total of 28 BMs found in these patients. The mean diameter of 28 BMs was 9,7 mm. The other 15 metastatic lesions could not be seen using 18F-FDG PET/CT, despite 13 of the 28 metastatic lesions being detected. Of the 13 lesions detected by 18F-FDG PET/CT, 4 (30.8%) were hypometabolic, 6 (46.2%) were hypermetabolic, and the remaining 3 (23.0%) were mixed. Table 2 summarizes the appearance patterns of BMs on 18F-FDG PET/CT.

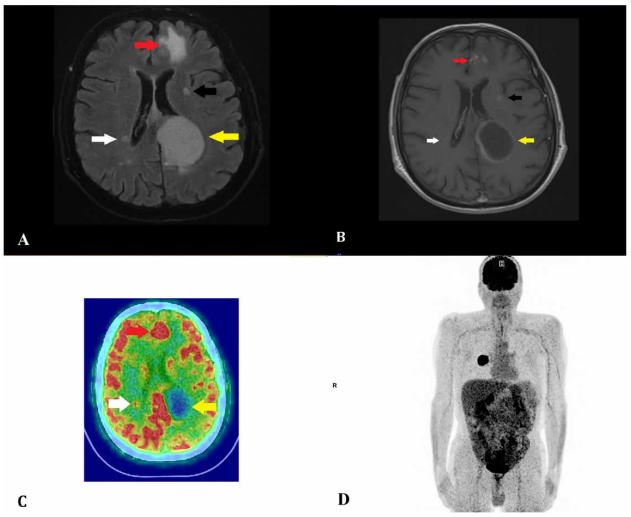

Fig. 1 Periventricular metastatic nodular lesions with contrast enhancement were observed in FLAIR (A) and postcontrast T1W (B) sequences on MRI. Representative PET images (C) show that lesions marked with red and white arrows are hypermetabolic and the lesion marked with yellow arrows has a mixed pattern. The lesion marked with a black arrow on MRI images cannot be detected on 18F-FDG PET/CT. D shows the coronal maximum intense projection image of small cell lung cancer with the right perihilar location.

18F-FDG PET/CT detected BMs with a mean diameter of 16 mm. The smallest BM found was 8 mm in diameter, whereas the unidentified lesions had a mean diameter of 4.3 mm. Regarding 18F-FDG PET/CT, 10 of the 11 patients with BMs were also advanced-stage patients. When staged according to 18F-FDG PET/CT, the remaining one patient, whose BMs were discovered with MRI but not with 18F-FDG PET/CT, was in the limited stage. One patient was in the advanced stages of the disease, with isolated BM visible on 18F-FDG PET/CT and MRI.

Discussion

Due to their small size, more than half of the BMs did not show any imaging results on 18F-FDG PET/CT in this study. Furthermore, the metabolic natures of BMs with 18F-FDG PET/CT imaging findings were discovered to have diverse looks.

The incidence of BMs at the initial diagnosis was 21.6% in this study. This rate was similar to what was shown in the literature. Moreover, the detectability rate of 18F-FDG PET/CT for BMs was 47.3%, which was consistent with earlier research (5, 10). According to a study that evaluated all types of lung cancer without discrimination, 18F-FDG PET/CT has a sensitivity of 72% for detecting BMs (11). The reason for this high rate may be that 18F-FDG PET/CT data were obtained up to three months after diagnosis. Although 18F-FDG PET/CT outperforms other imaging methods in determining the most metastatic areas, it falls short of brain MRI in detecting BMs (10). As is generally known, MRI has the best diagnostic performance when it comes to detecting abnormalities in the central nervous system (3).

BMs were found in 13 of 91 patients evaluated for BMs using CT and MRI in a research conducted by Brink et al. In six of the 13 patients, 18F-FDG PET/CT indicated BMs (10). In another study, BMs were detected by 18F-FDG PET/CT in five of 11 patients with BM. (5). One of the factors for the low detection rate is the insufficient resolution of 18F-FDG PET/CT in detecting small-sized BMs (12, 13). While the smallest detected lesion by 18F-FDG PET/CT in our series was 8 mm, the undetectable lesions had a mean diameter of 4.3 mm. These undetectable lesion dimensions are significantly below the spatial resolution limit of 18F-FDG PET/CT.

According to 18F-FDG PET/CT, one patient was in a limited stage, nevertheless, he was upstaged due to an isolated BM with a 5 mm diameter detected on brain MRI. Similarly, one patient in each of the investigations by Brink et al. and Vinjamury et al. was reported to have been upstaged due to a similar reason (5, 10). Another reason for the failure to detect BMs is the brain's high physiological FDG accumulation (14).

Radiotracers based on amino acid metabolism (18F-FDOPA, 18F-FET, and 11C-methionine) have surpassed 18F-FDG in identifying BMs over the previous decade, however, their specificities are lower than expected (15). For the identification of BMs, high-resolution detectors and novel radiopharmaceutical agents with a low tumor background rate are required. Many benign or malignant diseases of the brain can now be detected more precisely using PET/MRI scanners thanks to technological advances. Another factor to consider is that CT scanning in PET/CT is performed with a low dose of radiation and without the use of contrast material. It may be possible observe lesions and even recognize lesions without metabolic changes using contrast material and the diagnostic protocol dose of CT (16).

In SCLC, solely a few studies have analyzed the appearance of BMs on 18F-FDG PET/CT (6-8). Muñoz et al. determined that the appearance patterns of 8 BMs observed with 18F-FDG PET/CT in three patients were as follows: 6 hypometabolic, 1 hypermetabolic, and 1 mixed pattern (6). With 18F-FDG PET/CT, we were able to detect 13 BMs in this investigation. There were 4 hypometabolic lesions, 6 hypermetabolic lesions, and 3 mixed lesions. The fact that the lesions have various metabolic natures assists explain their diverse appearances (7). Mixed patterns are also caused by variables such as peritumoral edema and intratumoral necrosis. Traumas, primary malignancies, or infectious pathologies may lead to these appearances (7). To avoid being influenced by these factors, strict inclusion criteria were developed in this study.

The retrospective design, the single-centre experience, and the lack of histopathologically verified BMs are all limitations of the study. Another issue was that our study did not evaluate the MRI appearances of suspicious brain lesion findings on 18F-FDG PET/CT as the major

goal of this study was to investigate how metastases detected by brain MRI appeared on 18F-FDG PET/CT.

Conclusion

Owing to their metabolic nature, BMs may appear differently on 18F-FDG PET/CT. Due to these differences in appearance, caution should be exercised when interpreting BMs with 18F-FDG PET/CT. However, the failure of 18F-FDG PET/CT to detect small BMs prevents proper staging in SCLC.

References

1.Ko J, Winslow MM, Sage J. Mechanisms of small cell lung cancer metastasis. EMBO Mol Med 2021; 13(1): e13122. 2020/12/10.

2.Rittberg R, Banerji S, Kim JO, Rathod S, Dawe DE. Treatment and Prevention of Brain Metastases in Small Cell Lung Cancer. Am J Clin Oncol 2021; 44(12): 629-38. 2021/10/11.

3.Hochstenbag MM, Twijnstra A, Wilmink JT, Wouters EF, ten Velde GP. Asymptomatic brain metastases (BM) in small cell lung cancer (SCLC): MR-imaging is useful at initial diagnosis. J Neurooncol 2000; 48(3): 243-8. 2000/12/02.

4.Lu YY, Chen JH, Liang JA et al. 18F-FDG PET or PET/CT for detecting extensive disease in small-cell lung cancer: a systematic review and meta-analysis. Nucl Med Commun 2014; 35(7): 697-703. 2014/04/04.

5.Vinjamuri M, Craig M, Campbell-Fontaine A, et al. Can positron emission tomography be used as a staging tool for small-cell lung cancer? Clin Lung Cancer 2008; 9(1): 30-4. 2008/02/20.

6.Palomar Muñoz A, García Vicente AM, Bellón Guardia ME, et al. Is a selective brain (18)F-FDG PET/CT study profitable in patients with small cell lung cancer? Rev Esp Med Nucl Imagen Mol 2012; 31(3): 124-9. 2011/07/05.

7.Omuro AM, Leite CC, Mokhtari K, Delattre JY. Pitfalls in the diagnosis of brain tumours. Lancet Neurol 2006; 5(11): 937-48. 2006/10/21.

8.Lee HY, Chung JK, Jeong JM, et al. Comparison of FDG-PET findings of brain metastasis from non-small-cell lung cancer and small-cell lung cancer. Ann Nucl Med 2008; 22(4): 281-6. 2008/06/07.

9.Stahel RA, Ginsberg R, Havemann K, et al. Staging and prognostic factors in small cell lung cancer: a consensus report. Lung cancer 1989; 5(4-6): 119-26.

10.Brink I, Schumacher T, Mix M, et al. Impact of [18F]FDG-PET on the primary staging of small-cell lung cancer. Eur J Nucl Med Mol Imaging 2004; 31(12): 1614-20. 2004/07/20.

11.Hjorthaug K, Højbjerg JA, Knap MM, et al. Accuracy of 18F-FDG PET-CT in triaging lung cancer patients with suspected brain metastases for MRI. Nucl Med Commun 2015; 36(11): 1084-90. 2015/08/25.

12.Zimmer L, Luxen A. PET radiotracers for molecular imaging in the brain: past, present and future. Neuroimage 2012; 61(2): 363-70. 2012/01/10. doi: 10.1016/j.neuroimage.2011.12.037.

13.Fink KR, Fink JR. Imaging of brain metastases. Surg Neurol Int 2013; 4(Suppl 4): S209-19. 2013/05/30. doi: 10.4103/2152-7806.111298.

14.Kitajima K, Nakamoto Y, Okizuka H, et al. Accuracy of whole-body FDG-PET/CT for detecting brain metastases from non-central nervous system tumors. Ann Nucl Med 2008; 22(7): 595-602. 2008/08/30.

15.Juhász C, Dwivedi S, Kamson DO, Michelhaugh SK, Mittal S. Comparison of amino acid positron emission tomographic radiotracers for molecular imaging of primary and metastatic brain tumors. Mol Imaging 2014; 13. 2014/05/16.

16.De Wever W, Bruyeer E, Demaerel P, et al. Staging of lung cancer. Do we need a diagnostic CT of the brain after an integrated PET/CT for the detection of brain metastases? Jbr-btr 2010; 93(2): 71-6. 2010/06/09.